ISSN (Print) : 2320 – 3765
ISSN (Online): 2278 – 8875

International Journal of Advanced Research in Electrical, Electronics and Instrumentation Engineering

(An ISO 3297: 2007 Certified Organization)

Vol. 5, Issue 6, June 2016

Design & Analysis of Passive Damping LCL Filter for Power Quality Improvement Using SAPF Based on Artificial Intelligent Techniques

Dr. L.Ravi Srinivas[1], K. Sudha Rajesh[2]

Professor, Dept. of EEE, Gudlavalleru Engineering College (JNTUK Autonomous), Gudlavalleru, Andhra Pradesh, India[1]

PG Student [PEED], Gudlavalleru Engineering College (JNTUK Autonomous), Gudlavalleru, Andhra Pradesh, India[2]

ABSTRACT: This paper proposes and designs an new output filter for application to three phase three wire SAPF.This new output filter is derived from a traditional LCL filter by replacing its capacitor with C-tuned filter.This LCL filter can achieve high compensation bandwidth and low switching frequency current capability than traditional passive damping LCL filter.The LC branch serice resonant frequency of new LCL filter is set at the switching frequency, As a result, the power losses in the damping resistor of the new LCL filter can be reduced when compared to traditional passive damped LCL filters.The SAPF is used for harmonics and power compensation due to Non linear loads. The reference currents are generated with Enhanced SRF theory. The gating pulses for the switches in voltage source inverter of active filter are generated by hysteresis band current controller. DE,HDE and VSHDE habituated to tune the parameters of PI controller, to procure optimal solution. The effective simulations are carried out in MATLAB/Simulink.

KEYWORDS: Power Quality (PQ), Shunt Active Power Filter(SAPF), Hysteresis Band Current Controller (HBCC), Total Harmonic Distortion (THD), Differential Evolution(DE), Hybrid Differential Evolution(HDE), Variable Scaling Hybrid Differential Evolution (VSDHE).

I. INTRODUCTION

Voltage source converters (VSCs) have been widely used in many application fields, such as distributed generations , microgrids, shunt active power filters (SAPFs), adjustable speed drivers (ASDs), uninterruptible power supplies (UPS), etc. The proper implementation of close-loop current control schemes and pulse-width modulation (PWM) strategies in a VSC can insure good current output performance within its control bandwidth. However, the switching harmonic currents associated with the PWM process of the VSC still need to be attenuated by an output filter, otherwise they may cause harmonic interference and EMI problems in the grid or other facilities.

The output filter or grid interface filter of a VSC is essential to its output current quality. Traditionally, an inductor is connected at the ac output terminal of a VSC as an interface filter. However, a high inductance is required to obtain good harmonic attenuation performance, which may affect the dynamic characteristic and cause an over-modulation problem. An LCL filter is a better solution than an L filter, because it can attenuate high-frequency harmonic well with a smaller output inductance and a reduced size and cost. However, a serious challenge faced by the LCL filter is its resonance problem, which may make the whole system unstable and degrade the output performance of the VSC. Fortunately, this LCL filter resonance problem can be solved with different damping methods, which can be classified as passive damping and active damping.

Passive damping is implemented by adding some passive components to the original LCL filter . Different passive damping configurations of the LCL filter are shown in Fig. 1(b) shows the single resistor passive damping method of the LCL filter, in which a damping resistor R_d is connected in series with the filter capacitor c_1. This method

ISSN (Print) : 2320 – 3765
ISSN (Online): 2278 – 8875

International Journal of Advanced Research in Electrical, Electronics and Instrumentation Engineering

(An ISO 3297: 2007 Certified Organization)

Vol. 5, Issue 6, June 2016

is simple and straightforward, but the power losses of the damping resistor may be very high and will decrease the overall system efficiency. Moreover, the switching harmonic attenuation performance of the LCL filter may be degraded by the passive damping. Therefore, it is desirable to find some other passive damping solutions with less power losses for the LCL filter, such as those shown as Fig. 1 (c)-(d). These methods are basically focused on reducing low frequency power losses. This is done by reducing the fundamental currents that flow through the damping resistor. Meanwhile, the switching harmonic attenuation performance may be affected.

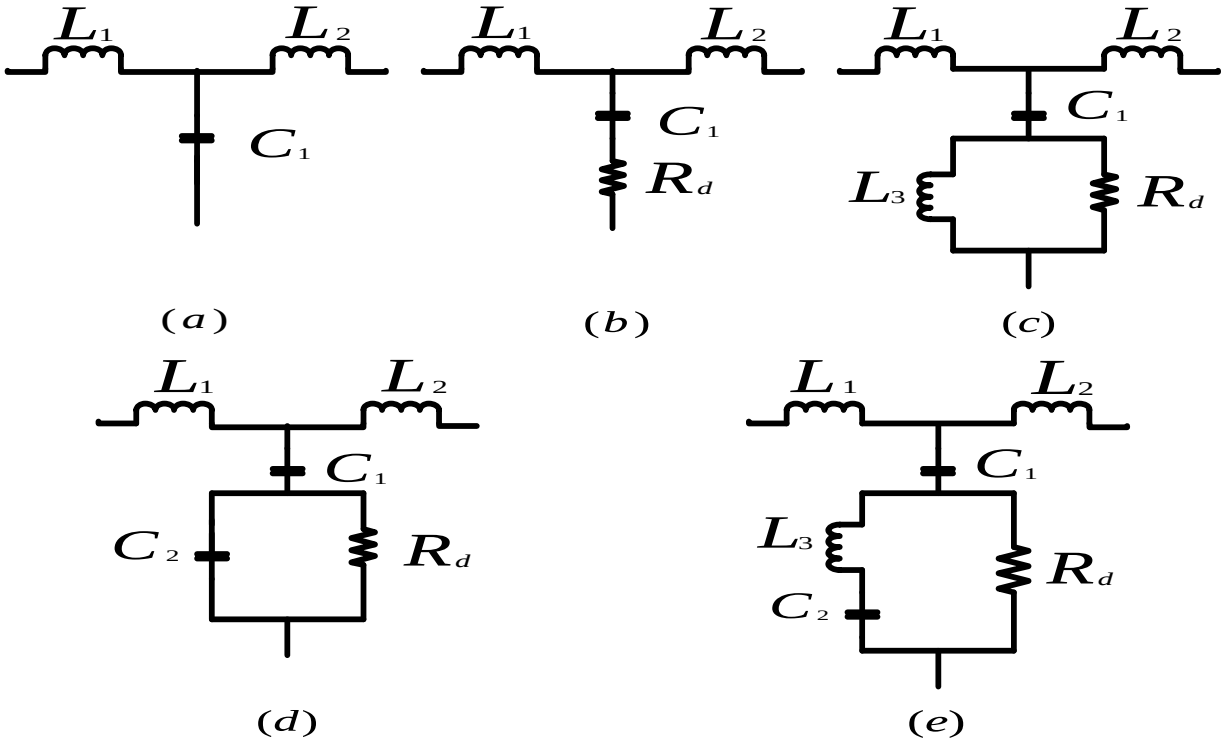

Fig 1: Different passive damping configurations of LCL filter.

This paper proposes and designs an new output filter for application to a three phase three wire SAPF. This new output filter is derived from a traditional LCL filter by replacing its capacitor with a C-type filter . It must be noted that the C-type filter adopted in the LCL filter is not the same as that commonly referred to in the literature. Traditionally, C-type filters have been mainly used as independent passive power filters (PPFs) in industrial applications fields, such as iron and steel plants , and so on. There are also papers that discuss the applications of a C-type filter together with an APF. However, in those papers, the C-type filters are connected in series or parallel with the APF to form hybrid filters, whose main purpose is reducing the rating of the APF. In this paper, the C-type filter based LCL filter is an indivisible component of the SAPF, and it plays an important role in sweeping out the switching harmonic from the SAPF output current.

The design of Shunt active power filter purpose is to elimination of harmonics for wide range of variation of load current under difference non-linear load. Therefore the Enhanced SRF theory yields an improved total harmonic distortion performance compared with hysteresis band current control method. The further optimization techniques is suitable for Enhanced SRF theory controlled Shunt active power filter is DE,HDE and VSHDE. It is used to alleviate the total harmonics distortion compared to Enhanced SRF theory controller.

The variable scaling factor based on the 1/5 success rule is used in the variable scaling hybrid differential evolution method to overcome the disadvantage of the random scaling factor and fixed scaling factor and reduce the problem of the selection of a mutation operation in the hybrid differential evolution.

ISSN (Print) : 2320 – 3765
ISSN (Online): 2278 – 8875

International Journal of Advanced Research in Electrical, Electronics and Instrumentation Engineering

(An ISO 3297: 2007 Certified Organization)

Vol. 5, Issue 6, June 2016

II. SHUNT ACTIVE POWER FILTER

Shunt active power filter configuration is chosen. The active power line conditioner is connected in parallel with the load being compensated at Point of Common Coupling (PCC). For this power circuit, a Pulse Width Modulation (PWM) based two-level voltage source inverter is in use, which operates in a current control mode. The current compensation is performed in time domain approach (specification) for faster response. The purpose is to inject the compensating current at the parallel point such that the source current becomes sinusoidal, since this shunt active power line conditioner is used for cancelling the current harmonics.

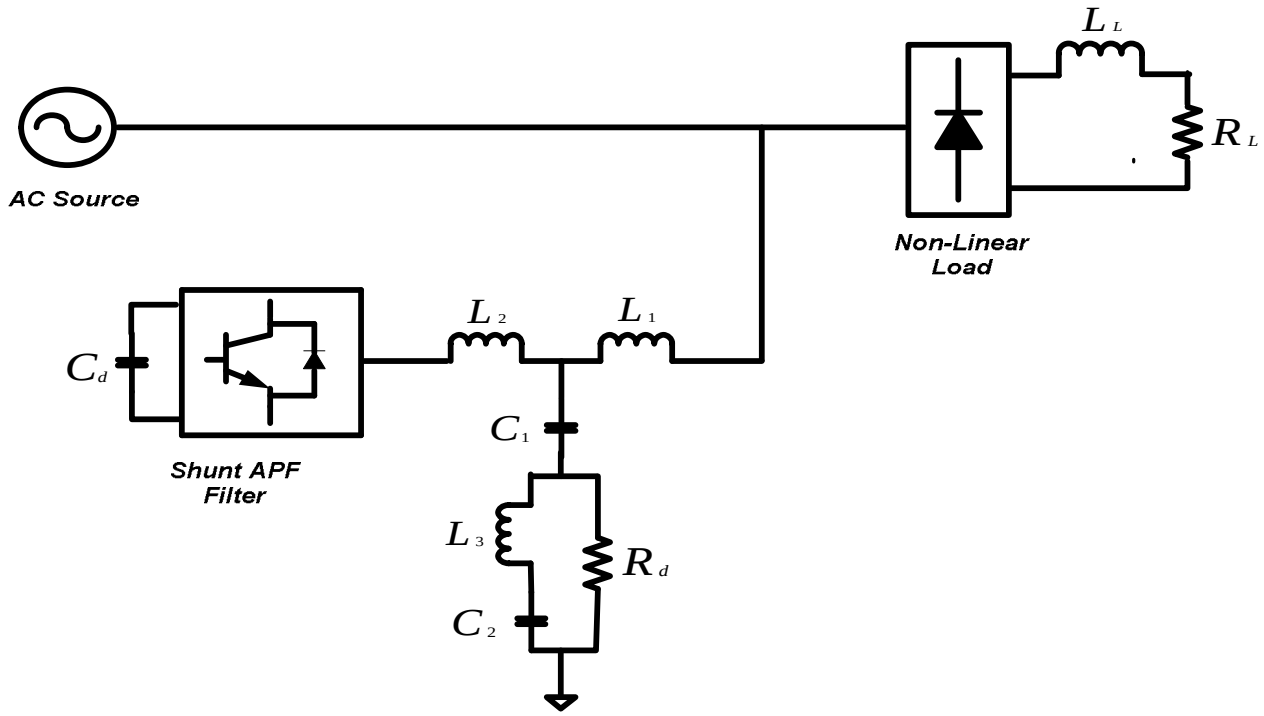

Fig 2:Single line diagram of SAPF with output LCL filter connected to line

VSI DESIGN:

The PWM-VSI is assumed to operate in the linear modulation mode ($0 \leq m_a \leq 1$) , and then the amplitude modulation factor m_a is calculated as

DC bus Voltage of the APF:

$$V_{dc_{APF}} = \frac{2\sqrt{2} * V_f}{m_a} \quad m_a = 0.9$$

$$= 689.486 \quad \approx \mathbf{700V}$$

DC Bus capacitance of the APF:

$$C_{dc} = \frac{6 V_f I_f \Delta t}{(V_{dc}^2 - V_{dcmin}^2)} = \mathbf{0.087691326\ F}$$

ISSN (Print) : 2320 – 3765
ISSN (Online): 2278 – 8875

International Journal of Advanced Research in Electrical, Electronics and Instrumentation Engineering

(An ISO 3297: 2007 Certified Organization)

Vol. 5, Issue 6, June 2016

III. DESIGN OF THE LCL FILTER

The single-phase equivalent topology of the proposed LCL filter that is shown in Fig. 3(b). For comparison, the traditional passive damped LCL filter is shown in Fig. 3(a).

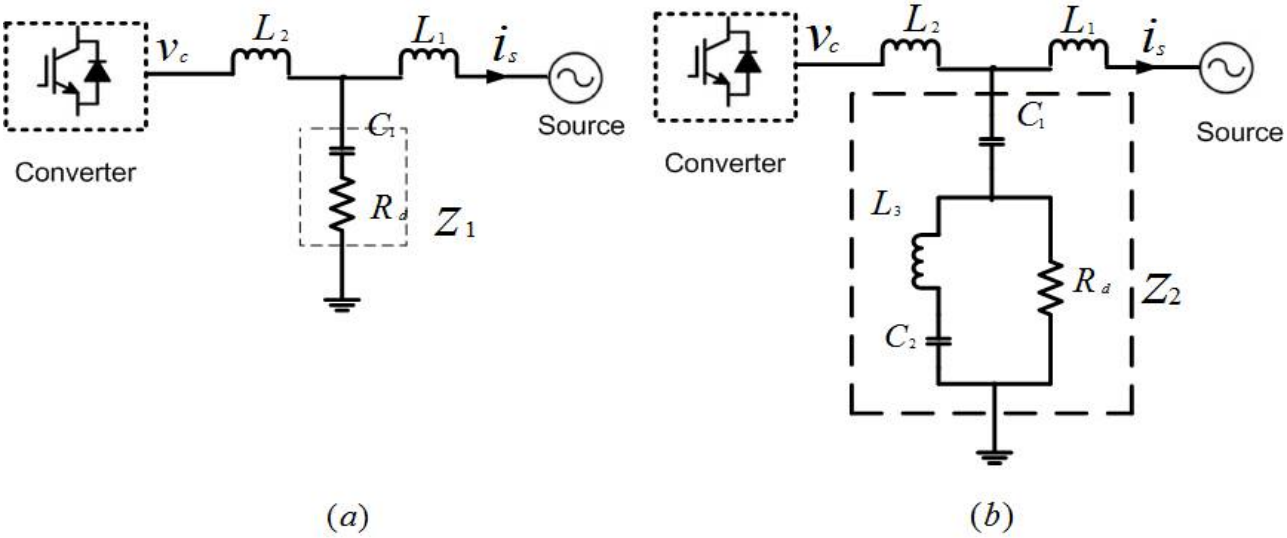

Fig 3: Single-phase equivalent topologies of SAPFs with (a) the traditional LCL filter, (b) the proposed LCFL filter.

The C-type filter is in the dashed line box shown in Fig.3(b), where Z_2 is the impedance of the C-type filter, which can be written as:

$$Z_2 = \frac{S^3(C_1C_2L_3R_d)+S^2(C_2L_3)+S(R_d(C_1+C_2))}{S^3L_3C_2+S^2C_1C_2R_d+SC_1}$$

The impedance of its RC series branch from fig.3(a), which can be written as:

$$Z_1 = R_d + \frac{1}{C_1S} = \frac{R_d+C_1S}{C_1S}$$

The transfer function of the LCL filter with RC series branch

$$\frac{I_S}{V_C} = \frac{R_d+SC_1}{S^3L_1L_2C_1+S^2C_1(L_1+L_2)+SR_d}$$

Transfer function For LCL filter with C-Tuned filter

$$\frac{I_S}{V_C} = \frac{S^3(C_1C_2L_3R_d)+S^2(C_2L_3)+SR_d(C_1+C_2)+1}{S^5L_1L_2L_3C_1C_2+S^4C_1C_2R_d(L_1L_2+L_1L_3+L_2L_3)+S^3(L_1L_2C_1+L_1L_3C_2+L_2L_3C_2)+S^2R_d(L_1+L_2)(C_1+C_2)+S(L_1+L_2)}$$

From the above transfer functions bode plot is drawn for different LCL filters and there response shown in next page.

ISSN (Print) : 2320 – 3765
ISSN (Online): 2278 – 8875

International Journal of Advanced Research in Electrical, Electronics and Instrumentation Engineering

(An ISO 3297: 2007 Certified Organization)

Vol. 5, Issue 6, June 2016

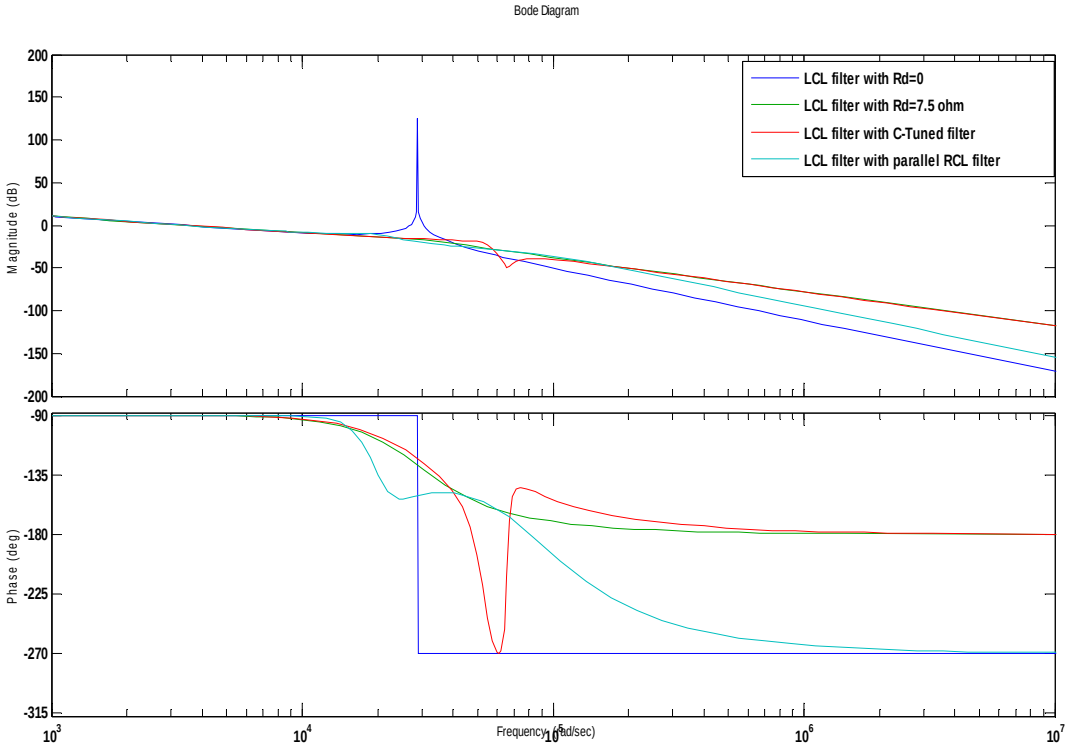

Fig 4: Bode plots of the LCL filters.

The LCL filter can be designed by the following step-by-step design procedure.

1) Select the output inductors L_1 *and* L_2

The total output inductance cannot be too high, since it will increase the voltage drop along the inductor and affect the reference current tracking ability of the SAPF. However, if the output inductance is too small, its current ripple attenuation performance may be degraded.

Maximum output inductance that satisfies the current reference tracking demand can be obtained as:

$$L \leq \frac{(u_l + {}^{2V_{dc}}/_{3})}{\Delta i^*_{max}} T_s \qquad (4.1)$$

Minimum output inductance that satisfies the current ripple alleviation demand can be obtained as:

$$L \geq \frac{(2V_{dc} - 3u_l)T_s u_l}{2V_{dc}\Delta i_{ripp}} \qquad (4.2)$$

Based on above equation-4.1,equation-4.2, the total output inductance value range can be determined as:

$$\frac{(2V_{dc} - 3u_{sa})T_s u_{sa}}{2V_{dc}\Delta i_{ripp}} \leq L \leq \frac{(u_{sa} + {}^{2V_{dc}}/_{3})}{\Delta i^*_{max}} T_s \qquad (4.3)$$

Where $V_{dc} = 700V$, $u_{sa} = 311V, T_s = 1/9600s, i^*_{max} = 100\sqrt{2}A,$ *and* $\Delta i_{ripp} = 20A.$ *By*

Substituting these parameters into equation-4.3 the total output inductance value range of the LCL filter can be obtained as:

$$208\mu H \leq L \leq 555\mu H.$$

- Let $L_2 = a_1 * L_1$. Then, we have, L=$\frac{(1+a_L)^2}{\omega_r^2 a_L C}$
- L is minimum when, $dL/da_L = 0$ *and* $d^2L/da_L^2 > 0$. This gives $a_L = 2$
- Lowest ripple current in the output for a given L and ω_r occurs at $L_2 = 2 * L_1$.
- Chosen values of $L_1 = 100\,\mu H$ *and* $L_2 = 200\,\mu H$.

ISSN (Print) : 2320 – 3765
ISSN (Online): 2278 – 8875

International Journal of Advanced Research in Electrical, Electronics and Instrumentation Engineering

(An ISO 3297: 2007 Certified Organization)

Vol. 5, Issue 6, June 2016

2) Determine the filter capacitor C_1

The resonance frequency of the output filter of the SAPF must satisfy the constraint of:

$$\frac{f_{max}}{0.3} \leq f_{res} = \frac{1}{2\pi}\sqrt{\frac{L_1+L_2}{L_1L_2C_1}} \leq \frac{f_{sw}}{2}$$

Where f_{max} is highest frequency of harmonic current that needs to be compensated by the SAPF, and f_{sw} is the switching frequency of the SAPF converter .

Therefore, the value range of the filter capacitance C_1 can be calculated from equation- as:

$$16.5\mu F \leq C_1 \leq 21.9\mu F$$

The filter capacitance was chosen as C_1=18μF, and the resonant frequency was verified by:

$$f_{res} = \frac{1}{2\pi}\sqrt{\frac{L_1+L_2}{L_1L_2C_1}} = \frac{10^6}{2\pi\sqrt{66.6*18}} = 4.59kHz$$

Which falls into the range from 4.17 to 4.8kHz

3) Choose the damping resistor R_d.

Passive damping must be sufficient to alleviate resonance at a frequency of f_{res}, Meanwhile, its power losses cannot be too high. The damping resistance is set to a value similar to that of the filter capacitor impedance at the resonance frequency,

$$|Z_{cf}|_{f_{res}} = \frac{1}{2\pi f_{res}c_1} \approx 1.96\,\Omega.$$

The damping resistance was chosen as $R_d = 2.5\,\Omega$

4) Choose the LC series branch L_3 *and* C_2

The series resonance frequency of the LC branch must be tuned at around the switching frequency to bypass the switching current, which can be calculated as:

$$f_{LC} = \frac{1}{2\pi\sqrt{L_3C_2}} \approx 9.6kHz$$

The LC branch capacitance is chosen as $C_2 = 3\mu F$ *and* then the LC branch inductance can be calculated from above equation as $L_3 \approx 90\mu H$

Subsystems	Quantity	values
AC Source	Source voltage V_s	380 V
	Line frequency f_n	50 Hz
	Source impedance L_s	100 μH
SAPF converter	Nominal power	66 kVA
	Switching frequency f_s	9.6kHz
	DC bus voltage V_{dc}	700 V
LCFL filter (delta connection)	Source side inductor L_1	100μH
	Converter side inductor L_2	200μH
	Filter capacitor C_1	6μF
	LC branch inductor L_3	270μH
	LC branch capacitor C_2	1μF
	Damping resistor R_d	7.5 Ω
LCL filter (delta connection)	Source side inductor L_1	100μH
	Converter side inductor L_2	200μH
	Filter capacitor C_1	6μF
	Damping resistor R_d	7.5 Ω
Nonlinear load	DC- link inductor L_l	0.5 mH
	DC- link resistor R_d	7.5 Ω

Table.1:Parameters

ISSN (Print) : 2320 – 3765
ISSN (Online): 2278 – 8875

International Journal of Advanced Research in Electrical, Electronics and Instrumentation Engineering

(An ISO 3297: 2007 Certified Organization)

Vol. 5, Issue 6, June 2016

IV.REFERENCE CURRENT CALCULATION

A. Proposed Enhanced-SRF

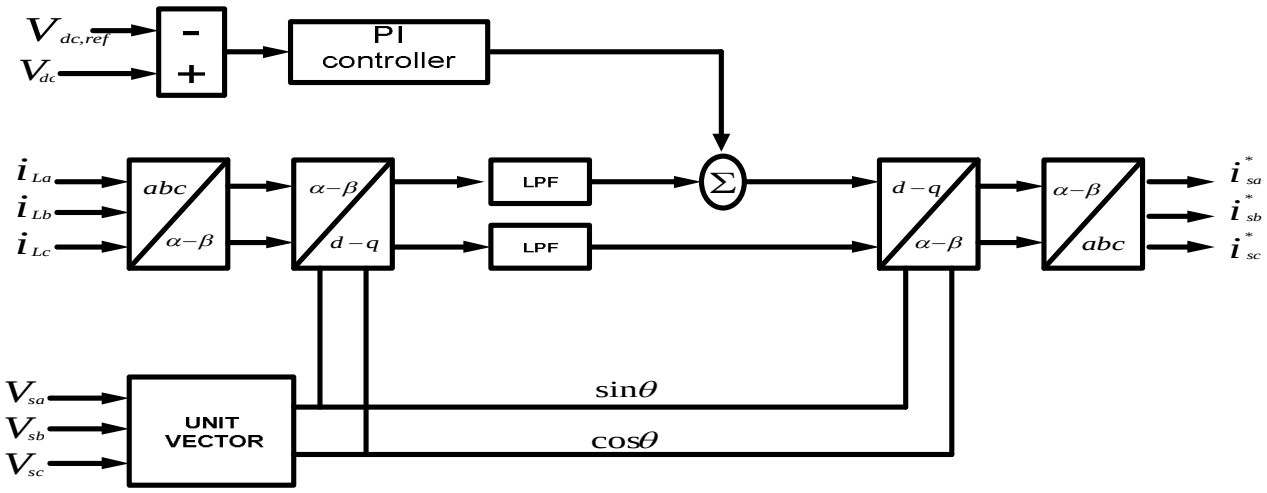

Fig.5: Block diagram of Enhanced SRF theory.

The block diagram of Enhanced-SRF structure is shown in Fig.5. The Enhanced-SRF method consist of simplified unit vector generation for vector orientation, dc-link capacitor voltage regulator and stationary-rotating synchronous frames to extract the reference current.

B. Unit vector generation

The simple and efficient unit vector generator is used for vector orientation. Fig.6 shows the block diagram of a unit vector generation method. To generate the synchronization vector the instantaneous supply voltages are sensed and computed.

The instantaneous three-phase source voltages are transformed into the two-phase stationary $\alpha - \beta$ voltages using Clarke transformation given in equation (2).Transforming equation (1) to $\alpha - \beta$ plane using equation (2) and simplifying,

$$\begin{aligned} V_{sa} &= V_{sm}\sin(\omega t) \\ V_{sb} &= V_{sm}\sin(\omega t - 120^0) \\ V_{sc} &= V_{sm}\sin(\omega t + 120^0) \end{aligned} \quad (1)$$

$$\begin{bmatrix} V_\alpha \\ V_\beta \end{bmatrix} = \sqrt{\frac{2}{3}} \begin{bmatrix} 1 & \frac{-1}{2} & \frac{-1}{2} \\ 0 & \frac{\sqrt{3}}{2} & \frac{-\sqrt{3}}{2} \end{bmatrix} \begin{bmatrix} V_{sa} \\ V_{sb} \\ V_{sc} \end{bmatrix} \quad (2)$$

$$\begin{aligned} V_{s\alpha} &= \frac{3}{2} V_m \sin(\omega t) \\ V_{s\beta} &= \frac{-3}{2} V_m \cos(\omega t) \end{aligned} \quad (3)$$

The voltages $\alpha - \beta$ are filtered using first order digital low pass filter whose frequency is ω(at fundamental frequency). After filtering, the percentage of h^{th} order harmonics of the sensed supply voltage are reduced by a factor of $\sqrt{2/(h^2+1)}$. It cancels the higher order harmonics, notches and high frequency noise. The estimated magnitude of the space vector generated is as follows

$$\overrightarrow{V} = \overrightarrow{V_{\alpha\beta}} = V_{s\alpha} + jV_{s\beta} = \sqrt{\left(V_{s\alpha}^2 + V_{s\beta}^2\right)} \quad (4)$$

ISSN (Print) : 2320 – 3765
ISSN (Online): 2278 – 8875

International Journal of Advanced Research in Electrical, Electronics and Instrumentation Engineering

(An ISO 3297: 2007 Certified Organization)

Vol. 5, Issue 6, June 2016

From the derivation in equation (4), it is evident that the unit vectors can be generated by transforming the supply voltage to $\alpha - \beta$ plane and dividing the $\alpha - \beta$ components by the magnitude of the space vector. Hence, the unit vector generation is defined as

$$\cos\theta = \frac{V_\alpha}{\sqrt{\left(V_{s\alpha}^2 + V_{s\beta}^2\right)}} = \frac{(3/2)V_m \sin(\omega t)}{(3/2)V_m} = \sin(\omega t)$$

$$\sin\theta = \frac{V_\beta}{\sqrt{\left(V_{s\alpha}^2 + V_{s\beta}^2\right)}} = \frac{-(3/2)V_m \cos(\omega t)}{(3/2)V_m} = -\cos(\omega t) \qquad (5)$$

This unit vector generation method results in elimination of supply harmonics, high frequency noise and notches in the distribution of supply voltages

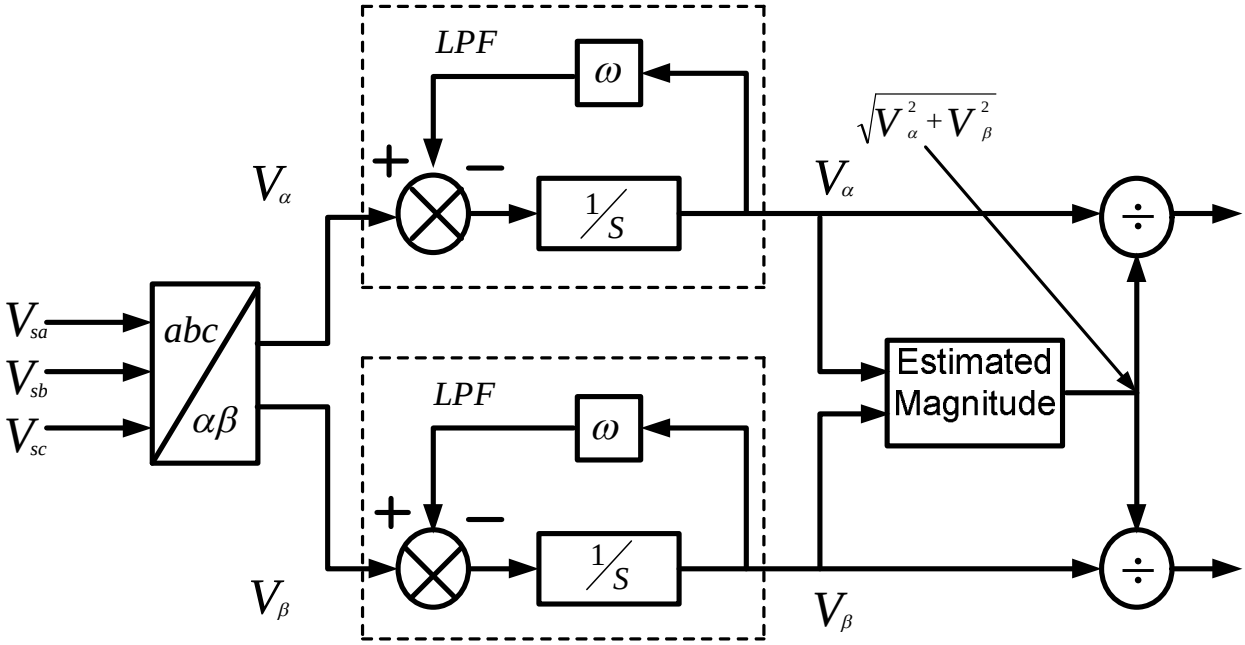

Fig.7:Block diagram of unit vector generator.

The conventional-SRF controller requires PLL-circuit for vector orientation. But the design of a high performance PLL-circuit is difficult and this drawback is rectified by the proposed Enhanced-SRF method. It uses a simple unit vector for vector orientation and $\alpha - \beta$ stationery frame transformation for high performance control strategy. The modified-SRF provides better performance than conventional method in terms of dc-voltage regulation, harmonic current elimination and reactive-power compensation.

C. Hysteresis Band Current Controller

A carrier less hysteresis band current controller is used over the reference currents (i_{sa}^*,i_{sb}^* and i_{sc}^*) and sensed supply currents (i_{sa}, i_{sb}, i_{sc}) to generate the switching signals for the MOSFETs of the current controlled VSI working as an active power filter. The switching signals are obtained as follows

If $i_{sx} > (i_{sx}^* + hb)$, upper switch of x^{th} leg is ON and lower switch is OFF, and

If $i_{sx} < (i_{sx}^* + hb)$, upper switch of x^{th} leg is OFF and lower switch is ON.

Where 'hb' is the hysteresis band current controller around the reference current at each phase and x =a, b, c which stands for three legs of PWM converter.

ISSN (Print) : 2320 – 3765
ISSN (Online): 2278 – 8875

International Journal of Advanced Research in Electrical, Electronics and Instrumentation Engineering

(An ISO 3297: 2007 Certified Organization)

Vol. 5, Issue 6, June 2016

In response to the switching signals generated by controller, active power filter shapes the source currents to sinusoidal and it compensates the source side harmonics of the nonlinear load.

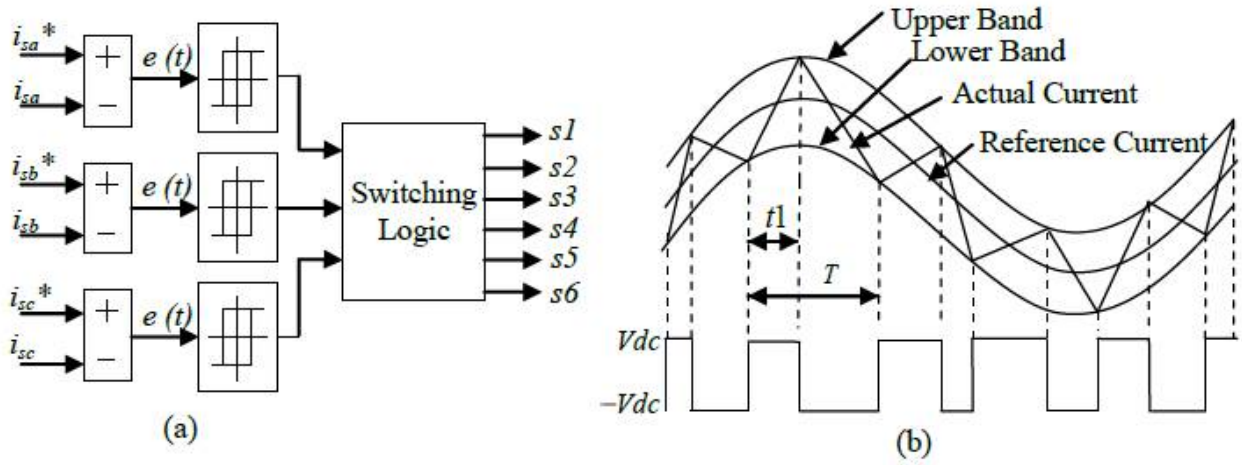

Fig.7: Hysteresis band current controller (a) Block diagram and (b)Wave form.

V.SIMULATION RESULTS

A simulation model of the studied hybrid active power filter is developed in MATLAB environment. The supply system used in 380V,3-phase, 50 Hz sinusoidal. The nonlinear system considered for compensation of diode rectifier with RL-load. Simulation results are obtained for both steady state and transient conditions. Different parameters used for simulation study are listed in Table.1.Fig.8 to Fig.13 show %THD of load current and source current for Enhanced SRF-controlled and PI- controlled shunt active power filters respectively. The source current is observed to be sinusoidal with power factor approaching unity, while the %THD in the source current is well below the IEEE 519 limits in both the cases. It is observed that the DC link voltage settles to a lower value in Enhanced SRF controlled SAPF as compared to PI- controlled SAPF, with lower transients in source current.

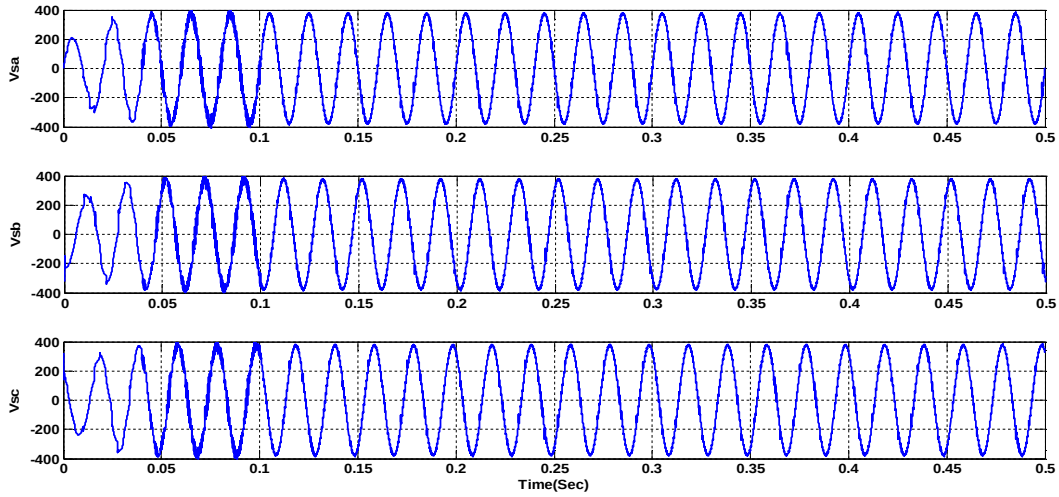

Fig.8: waveform of supply voltages V_{sa}, V_{sb}, and V_{sc} for Enhanced SRF control.

ISSN (Print) : 2320 – 3765
ISSN (Online): 2278 – 8875

International Journal of Advanced Research in Electrical, Electronics and Instrumentation Engineering

(An ISO 3297: 2007 Certified Organization)

Vol. 5, Issue 6, June 2016

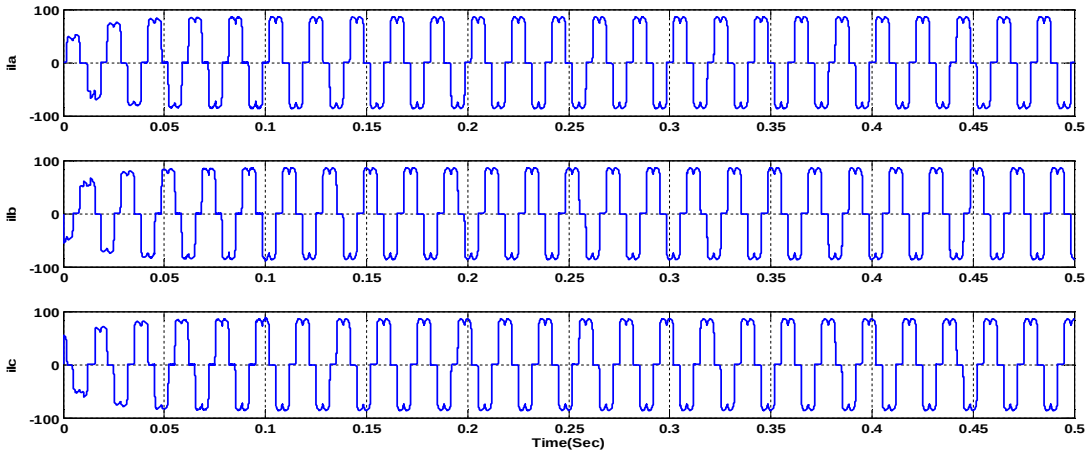

Fig.9: Waveform of load currents I_{La}, I_{Lb}, and I_{Lc} for Enhanced SRF.

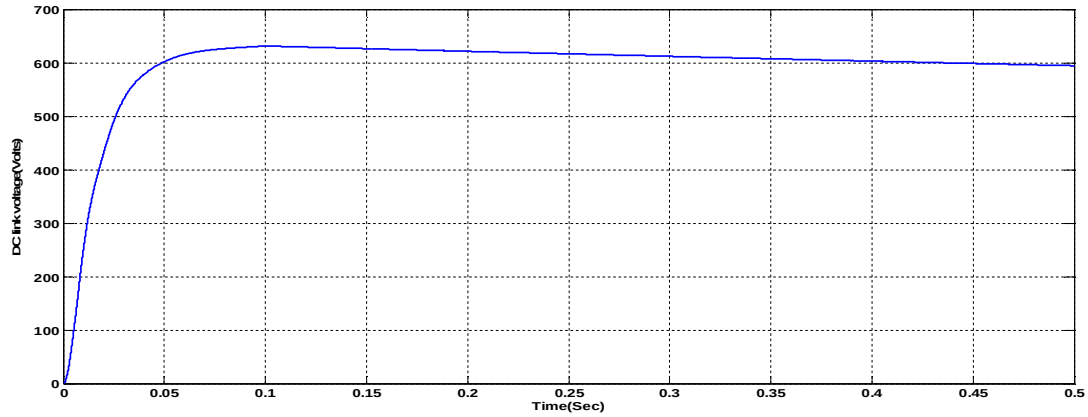

Fig 10: Waveform of DC voltage

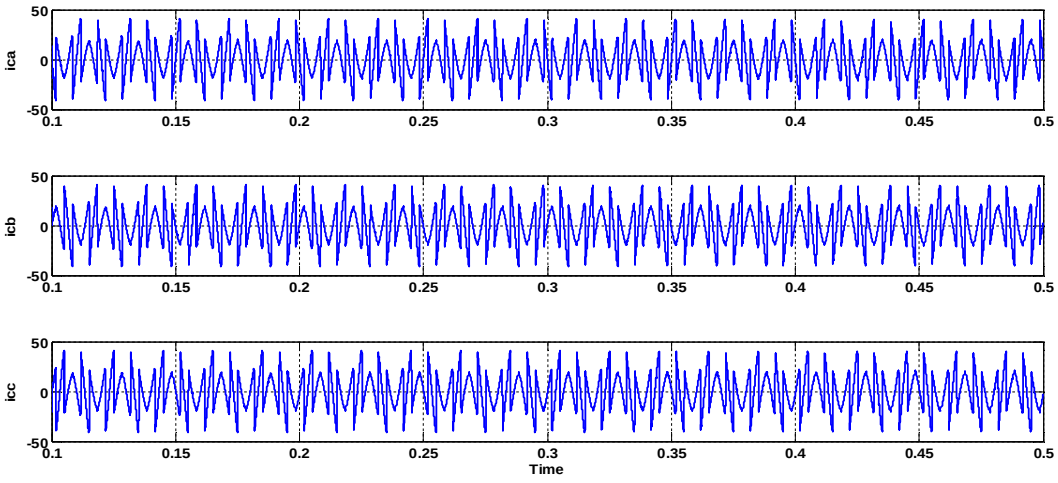

Fig.11: Waveform of compensating currents I_{ca}, I_{cb}, and I_{cc}.

ISSN (Print) : 2320 – 3765
ISSN (Online): 2278 – 8875

International Journal of Advanced Research in Electrical, Electronics and Instrumentation Engineering

(An ISO 3297: 2007 Certified Organization)

Vol. 5, Issue 6, June 2016

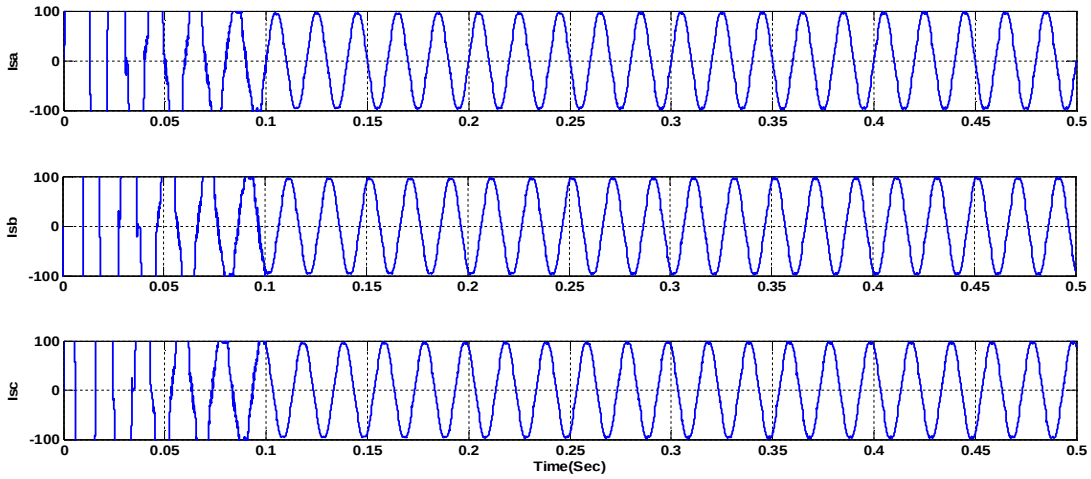

Fig.12: Waveform of source currents I_{sa}, I_{sb} and I_{sc} for Enhanced SRF controller.

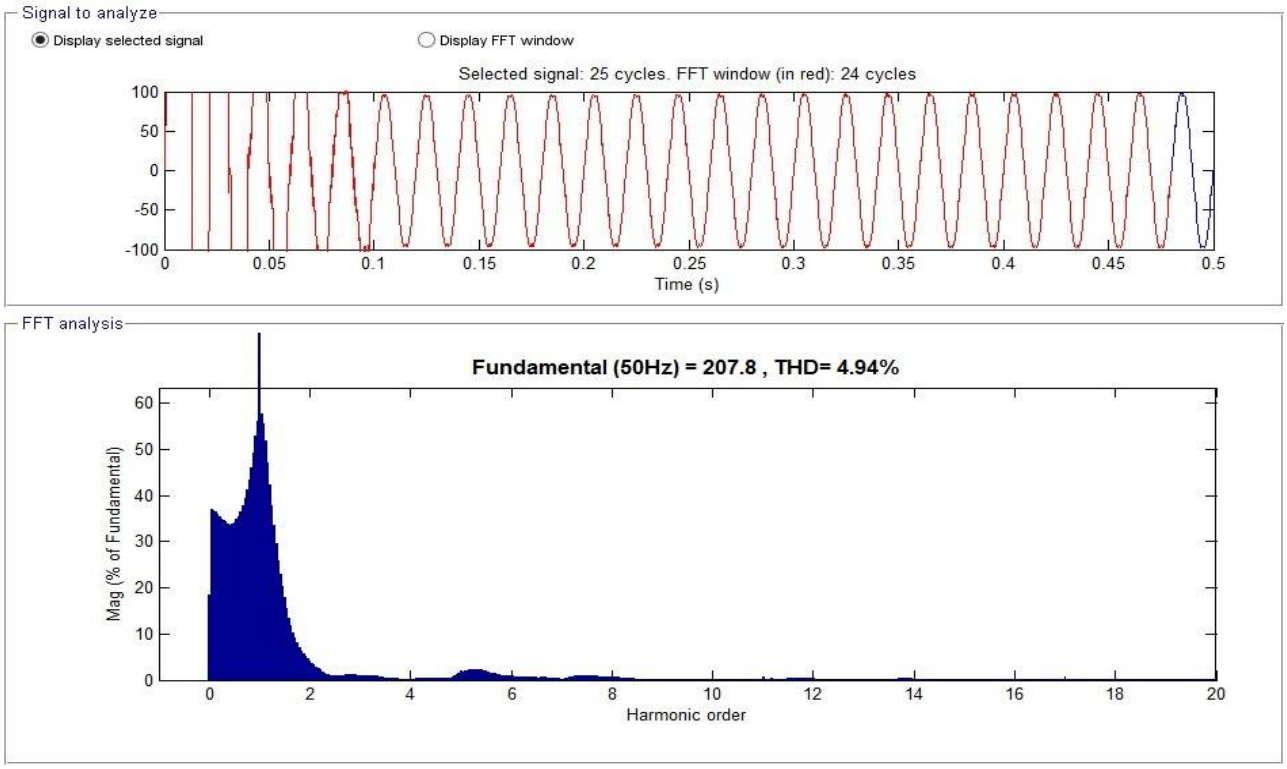

Fig.13: THD of supply current with designed Enhanced SRF controller.

The damping resistor power loss of the LCL filter can be calculated as $4.88^2 \times 7.5 = 164.26$(W), and the corresponding power loss of the C-type LCL filter is $3.413^2 \times 7.5 = 87.36$(W). It can be seen that the damping resistor power loss of the C-type LCL filter is much less than that of the traditional passive damped LCL filter.

ISSN (Print) : 2320 – 3765
ISSN (Online): 2278 – 8875

International Journal of Advanced Research in Electrical, Electronics and Instrumentation Engineering

(An ISO 3297: 2007 Certified Organization)

Vol. 5, Issue 6, June 2016

VI.VSHDE ALGORITHM

The variable scaling factor is used in VSHDE to overcome the drawback of the fixed and random scaling factor and alleviate the problem of selection of mutation operator in HDE. The rule of updating a scaling factor based on the 1/5 success rule of the ESs is used to adjust the scaling factor. The 1/5 success rule emerged as a conclusion of the process of optimizing convergence rate of two functions (the so-called corridor mode and sphere model). The rule of updating scaling factor is as follows:

$$F^{t+1} = \begin{cases} c_d * F^t, & \text{if } P_s^t < \frac{1}{5} \\ c_i * F^t, & \text{if } P_s^t > \frac{1}{5} \\ F^t, & \text{if } P_s^t = \frac{1}{5} \end{cases}$$

Where P_s^t is the frequency of successful mutations measured. The successful mutation defining the fitness value of the best individual in the next generation is better than the best individual in the current generation.$C_d = 0.82$ and $C_j = {}^1/_{0.81}$ The initial value of the cross over value is set to 0.6 to 0.9. The crossover value of CR= 0.6 and are used for adjustment, which should take place in every q iterations. The iteration index suggested by is equal to 10×b, where is a b constant. When the migration operator is performed, the value of scaling factor is defined as follows:

$$F = 1 - \frac{\text{iter}}{\text{iter max}}$$

Where iter and itermax are the number of current iteration and the maximum iteration, respectively. And, the scaling factor can be reset as when the scaling factor is too small to find better solution in the solution process. Formally, the variable scaling hybrid differential evolution algorithm is briefly described in the following:

Step1. Initialization

Input system data and generate the initial population. The initial population is chosen randomly and would attempt to cover the entire parameter space uniformly. The uniform probability distribution for all random variables as following is assumed.

$$X_i^G = X_{i,min} + rand_i[0,1](Z_{i,max} - Z_{i,min}), \quad i = 1, \ldots, N_p$$

Where $rand_i \in [0,1]$ is a random number. The initial process can produce N_p individuals of $\mathbf{X_i^G}$ randomly.

Step 2. Mutation operation

The essential ingredient in the mutation operation is the difference vector. Each individual pair in a population at the G^{th} generation defines a difference vector D_{jk} as

$$D_{jk} = X_j^G - X_k^G$$

The mutation process at G^{th} generation begins by randomly selecting either two or four population individuals X_j^G, X_k^G, X_l^G and X_m^G for any j, k, l and m. These four individuals are then combined to form a difference vector D_{jklm} as

$$D_{jklm} = D_{jk} + D_{lm} = (X_j^G - X_k^G) + (X_l^G - X_m^G)$$

A mutant vector is then generated based on the present individual in the mutation process by

$$X_i^{G+1} = X_p^G + F.D_{jklm}, i = 1,2, \ldots, N_p$$

ISSN (Print) : 2320 – 3765
ISSN (Online): 2278 – 8875

International Journal of Advanced Research in Electrical, Electronics and Instrumentation Engineering

(An ISO 3297: 2007 Certified Organization)

Vol. 5, Issue 6, June 2016

Where scaling factor, F is a constant. And, j, k, l and m are randomly selected. The perturbed individual it is essentially a noisy replica of X_p^G. Herein, the parent individual X_p^G depends on the circumstance in which the type of the mutation operations is employed.

Step 3. Crossover operation

In order to extend the diversity of further individuals at the next generation, the perturbed individual of X_i^{G+1} and the present individual of X_i^G are chosen by a binomial distribution to progress the crossover operation to generate the offspring.Each gene of i^{th} individual is reproduced from the mutant vectors

$X_i^{G+1} = [X_{1i}^{G+1}, X_{2i}^{G+1}, \ldots\ldots, X_{ni}^{G+1}]$and

the present individual

$$X_{gi}^{G+1} = \begin{cases} X_{gi}^{G}, & \text{if a random number} > cr \\ X_{gi}^{G+1}, & \text{otherwise} \end{cases}$$

Where, i = 1,...,N_p; g = 1,...,n; and the crossover factor Cr ∈ [0,1] is assigned by the user.

Step 4. Estimation and selection

The parent is replaced by its offspring if the fitness of the offspring is better than that of its parent. Contrarily, the parent is retained in the next generation if the fitness of the offspring is worse than that of its parent. Two forms are represented as follows:

$$X_i^{G+1} = \text{argmin}\{f(X_i^G), f(X_i^{G+1})\}$$

$$X_b^{G+1} = \text{argmin}\{f(X_i^G)\}$$

Step 5. Migrating operation

Migrating operation if necessary In order to effectively enhance the investigation of the search space and reduce the choice pressure of a small population, a migration phase is introduced to regenerate a new diverse population of individuals The new population is yielded based on the best individual X_b^{G+1}. The G^{th}gene of the i^{th} individual is as follows:

$$Z_{ig}^{G+1} = \begin{cases} X_{gi}^{G+1} + \text{rand}_i(X_{g\,min} - X_{bg}^{G+1}), & \text{if } \delta < \frac{X_{bg}^{G+1} - X_{g\,min}}{X_{g\,max} - X_{g\,min}} \\ X_{bg}^{G+1} + \text{rand}_i(X_{g\,min} - X_{bg}^{G+1}), & \text{otherwise} \end{cases}$$

Where $rand_i$ and δ are randomly generated numbers uniformly distributed in the range of [0,1]; i=1,. . .,N_p and g=1,. . .,n. The migrating operation is executed only if a measure fails to match the desired tolerance of population diversity. The measure is defined as follows:

$$\varepsilon = \sum_{\substack{i=1 \\ i \neq b}}^{N_p} \sum_{g=1}^{n} \frac{\eta Z}{n(N_{P-1})} < \varepsilon_1$$

$$\text{Where} \quad \eta Z = \begin{cases} 0, & \text{if } \varepsilon_2 < \left| \frac{X_{gi}^{G+1} - X_{bi}^{G+1}}{X_{bi}^{G+1}} \right| \\ 1, & \text{otherwise} \end{cases}$$

ISSN (Print) : 2320 – 3765
ISSN (Online): 2278 – 8875

International Journal of Advanced Research in Electrical, Electronics and Instrumentation Engineering

(An ISO 3297: 2007 Certified Organization)

Vol. 5, Issue 6, June 2016

Parameter $\varepsilon_1, \varepsilon_2$ [0,1] expresses the desired tolerance for the population diversity and the gene diversity with respect to the best individual. ηZ is the scale index. it can be seen that the value ε is in the range of [0,1]. If ε is smaller than ε_1, then the migrating operation is executed to generate a new population to escape the local point; otherwise, the migrating operation is turned off.

Step 6. Updating the scaling factor if necessary the scaling factor should be updated as in every q iterations. When the migrating operation performed or the scaling factor is too small to find the better solution, the scaling factor is reset.

Step 7. Repeat step 2 to step 6 until the maximum iteration quantity or the desired fitness is accomplished. The computational process of the VSHDE for solving economic dispatch systems is stated using a flowchart as shown in Fig.14

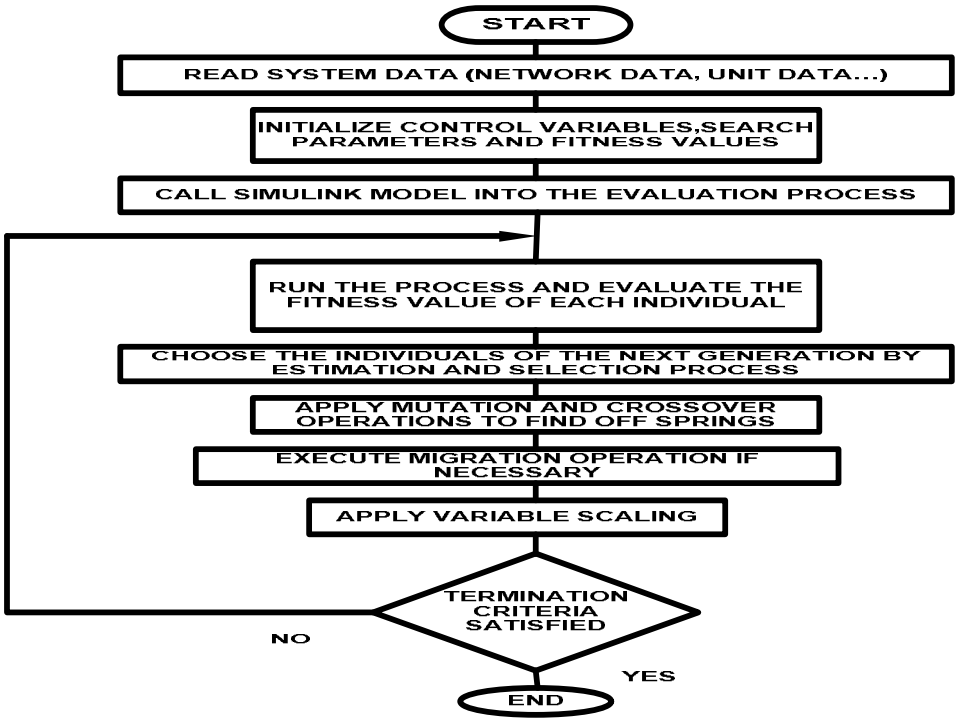

Fig.14:Flow chart diagram for VSHDE algorithm.

CONTROLLER	%THD	k_p	k_i
WITH PI	**4.31**	**0.00234**	**0.0090876**
WITH DE	**2.22**	**0.0600**	**0.0538**
WITH HDE	**2.17**	**0.0700**	**0.0616**
WITH VSHDE	**2.13**	**0.0636**	**0.0638**

Table 2: Relative comparison of Enhanced SRF controller, DE, HDE and VSHDE.

ISSN (Print) : 2320 – 3765
ISSN (Online): 2278 – 8875

International Journal of Advanced Research in Electrical, Electronics and Instrumentation Engineering

(An ISO 3297: 2007 Certified Organization)

Vol. 5, Issue 6, June 2016

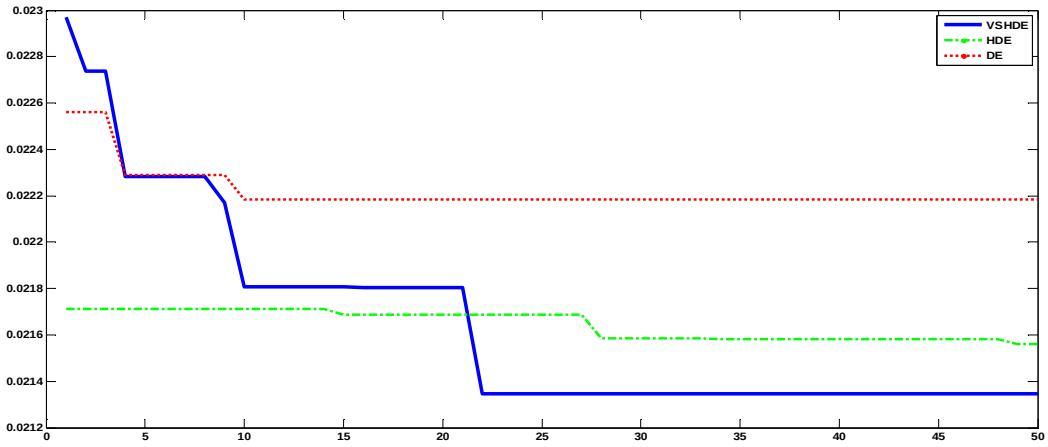

Fig 15: Convergence graph

VII.CONCLUSION

This paper proposed and designed an output filter called an new LCL filter for application to a three-phase three-wire SAPF. This new LCL filter is derived from a traditional LCL filter by replacing its capacitor with a C-type filter. Theoretical analyses have shown that the new LCL filter can provide better switching harmonic attenuation than the traditional passive damped LCL filter. Furthermore, since the switching harmonic currents are mostly bypassed by the LC series branch of the C-type filter, the damping resistor power loss can be significantly reduced by half when compared to the passive damped LCL filter. Comparative studies between the Enhanced SRF controller DE,HDE and VSHDE showed that VSHDE has been proved to be improved in terms of harmonic reduction in source currents. The dc bus voltage has been maintained constant equal to the reference voltage by Enhanced SRF control, VSHDE Optimization controllers.

REFERENCES

[1] Hou, Rui, et al. "Generalized design of shunt active power filter with output LCL filter." *Elektronika ir Elektrotechnika* 20.5 (2014): 65-71.
[2] Wu, Weimin, et al. "A new design method for the passive damped LCL and LLCL filter-based single-phase grid-tied inverter." *IEEE Transactions on Industrial Electronics* 60.10 (2013): 4339-4350.
[3] Muhlethaler, Jonas, et al. "Optimal design of LCL harmonic filters for three-phase PFC rectifiers." *IEEE Transactions on Power Electronics* 28.7 (2013): 3114-3125.
[4] Karuppanan, P. *Design and Implementation of Shunt Active Power Line Conditioner using Novel Control Strategies*. Diss. 2012.
[5] Pena-Alzola, Rafael, et al. "Analysis of the passive damping losses in LCL-filter-based grid converters." *IEEE Transactions on Power Electronics* 28.6 (2013): 2642-2646.
[6] Bina, M. Tavakoli, and E. Pashajavid. "An efficient procedure to design passive LCL-filters for active power filters." *Electric power systems research*79.4 (2009): 606-614.
[7] Storn, Rainer, and Kenneth Price. "Differential evolution–a simple and efficient heuristic for global optimization over continuous spaces." *Journal of global optimization* 11.4 (1997): 341-359.
[8] Chakraborty, Uday K., ed. *Advances in differential evolution*. Vol. 143. Springer, 2008.
[9] Chiou, Ji-Pyng, Chung-Fu Chang, and Ching-Tzong Su. "Variable scaling hybrid differential evolution for solving network reconfiguration of distribution systems." *IEEE Transactions on Power Systems* 20.2 (2005): 668-674.
[10] Gaing, Zwe-Lee. "A particle swarm optimization approach for optimum design of PID controller in AVR system." *IEEE transactions on energy conversion* 19.2 (2004): 384-391.